



ACCESS
Arctic Climate Change
Economy and Society



Project no. 265863

ACCESS

Arctic Climate Change, Economy and Society

Instrument: Collaborative Project
Thematic Priority: Ocean.2010-1 "Quantification of climate change impacts on economic sectors in the Arctic"

D4.55 – Report on the ocean properties of the Barents Sea region

Due date of deliverable: **31/08/2013**

Actual submission date: **01/10/2014**

Used Person/months: **13**

Start date of project: **March 1st, 2011**

Duration: **48 months**

Organisation name of lead contractor for this deliverable: **UPMC**

Project co-funded by the European Commission within the Seventh Framework Programme (2007-2013)		
Dissemination Level		
PU	Public	
PP	Restricted to other programme participants (including the Commission Services)	
RE	Restricted to a group specified by the consortium (including the Commission Services)	
CO	Confidential, only for members of the consortium (including the Commission Services)	X

Contents

Abstract	3
1. INTRODUCTION.....	4
1.1. The Barents Sea: A key region for water mass transformations and ventilation in the Arctic	4
1.2. Climate changes and long-term variability of the Barents Sea system	4
1.3. Problematic: What could be the Impacts of this warming trend and long-term ocean-ice-atmosphere variability on the Barents Sea water masses distribution?	5
1.4. Objectives.....	6
2. DATA AND METHOD	6
2.1. A new extensive hydrographic data set collection	6
2.2. Krigging : an optimal method for interpolating data.....	7
2.3. SINMOD 3-D Model Description and set-up (Slagstad, 1987)	7
3. RESULTS AND DISCUSSION.....	8
3.1. Summer Climatology from observations.....	8
3.1.1. Water masses.....	8
3.1.1.1. Theta-S diagrams analysis & main water mass definitions.....	8
3.1.1.2. Water mass occurrences.....	10
3.1.2. Description of the polar front structure	11
3.1.2.1. Vertical description of the polar front structure along the KOLA section... ..	11
3.1.2.2. Subsurface description of the 2D polar front structure.	12
3.2. Water Mass Variability in the atmosphere-ice-sea system context.....	13
3.2.1. From Observations	13
3.2.1.1. Changes in water types properties from Theta-S Diagram analysis: toward warmer and more saline AW	13
3.2.1.2. Water Mass Indexes: the “Atlantification” regime	14
3.2.2. From model	14
3.3. Variability of the fronts (SPF & NPF) : a model study.....	15
3.3.1. Comparison between two contrasted years: the cold 1998 and the “Atlantified” 2000. 16	16
3.3.2. Seasonality.....	16
4. CONCLUSION	16
Glossary of Acronyms.....	18
5. BIBLIOGRAPHY	18
FIGURES	21

Abstract

The Barents Sea (BS) is a transition area between the warm and saline Atlantic Waters (AW) and the cold and fresh Arctic Waters (ArW). A polar front structure separates the two water mass that will mix and cool to generate dense waters in winter. This study will use a new extensive hydrographic data set fulfilled by recent stations in the Russian area and a 3D coupled model as a back up to investigate the link between fronts and water masses, as well as their variability over the last 30 years. This study suggests that the polar front structure is composed of two branches and that the dense waters are found in between. The BS, especially in the East, is experiencing an “Atlantification” accompanied with a drastic sea ice decline. This changes, amplified during the last decade, shift the southern branch of the polar front structure in the North-East direction and affect negatively the dense water formation. This could have major impacts on climate by weakening the Arctic Ocean ventilation and on fisheries by shifting stocks in the Russian area.

ANNUAL AND INTERANNUAL VARIABILITY OF THE BARENTS SEA POLAR FRONT AND WATER MASSES: 1980-2010

Authors: Laurent Oziel¹ Dag Salgstad² Jean-Claude Gascard¹

¹ LOCEAN laboratory, University Pierre et Marie Curie, 4 Place Jussieu, 75252 Paris, Cedex 5.

² SINTEF Fisheries and Aquaculture, 7465 Trondheim, Norway.

1. INTRODUCTION

1.1. The Barents Sea: A key region for water mass transformations and ventilation in the Arctic

The Barents Sea (BS) is an Arco-boreal shelf (**Fig.1a**). Its latitudes range from 70°N up to 80°N and longitudes from 10°E to 65°E, covering around 1.4 million km², and its average depth is 230m. It is a key region for understanding water mass transformation in the Arctic because it is a pathway of the warm and saline Atlantic Waters (AW) flowing eastward and northward and mixing with the fresh and cold Arctic Waters (ArW) flowing westward and southward. BS is characterized by large hydrological contrasts. Salinity ranges between 33 psu and 35.2 psu due to very saline inflowing AW from the Norwegian Sea and fresh water contributions from the Norwegian Coastal Current Waters (NCCW), rivers and ice melting. The BS has also a large ocean temperature variation between -1.8°C for the ArW at depth (freezing point) and more than 10°C for the NCCW at surface during summer. Cooling and mixing of these water masses in the BS reinforced by brines rejections due to ice formation (especially in Svalbard, Franz Josef Land and Novaya Zemlya), produce locally the dense Barents Sea Waters (BSW). BSW, created by favorable conditions for shelf convection ([Martin and Cavalieri 1989](#)), mainly flow into the Arctic Ocean between Novaya Zemlya and Franz Josef Land and contribute for a part to the thermohaline overturning of the North Atlantic ([Anderson, Jones et al. 1999](#)). The densest BSW also provide intermediate waters to the Arctic Ocean to a depth of 1,200 m ([Rudels, Jones et al. 1994](#); [Schauer, Muench et al. 1997](#); [Schauer, Loeng et al. 2002](#)). Besides, the BS is very sensitive to and deeply involved in climate change.

1.2. Climate changes and long-term variability of the Barents Sea system

The BS experiences the largest sea ice decline in the Arctic ([Screen and Simmonds 2010](#)) which is a good indicator for the air-ice-ocean system variability ([Serreze, Holland et al. 2007](#)). For the last decade (1998-2008), BS annual Sea ice extent has decreased by 50% and has reached its lowest level for the last 60 years ([Årthun, Eldevik et al. 2012](#)). The BS is becoming one of the first “ice-free” Arctic Sea in autumn. In winter, a seasonal Marginal Ice Zone remains in the northern and sometimes eastern part of the BS close to Novaya Zemlya. The North-East BS is the most affected region by sea ice variability ([Inoue, Hori et al. 2012](#)).

With the sea ice decreasing, it is expected that the BS will interact more strongly with the atmosphere. The long-term variability of the BS as well as the whole Arctic appears to be partly associated with the Arctic Oscillation (AO) index, which is commonly given as a sea level air pressure and temperature index ([Thompson and Wallace 1998](#)). A negative AO generally corresponds to a cold atmospheric event, a high pressure and to an anticyclonic mode of the atmospheric circulation. A positive AO corresponds to a warm atmospheric event, a low pressure anomaly and a cyclonic atmospheric circulation. The AO decadal oscillation ([Proshutinsky and Johnson 1997](#)) affects the northern and eastern boundary conditions of the BS by forcing the AW flow through BSO and consequently the circulation in the BS. Indeed, a low pressure event (AO+) strengthens westerly winds in the inflow area and then increases the AW penetration in the BS ([Ingvaldsen 2004](#)). This would carry on more AW warm waters, decrease sea ice extent and enhance heat loss from the ocean to the atmosphere but increase fresh water content from ice melting.

An oceanic oscillation about 5-7 years period between cold and warm events was also mentioned by [Furevick \(2001\)](#). Impacts of this multi-annual oscillation on BS water mass transformations are still in debate. A warm and salty ocean might thus generate more dense water due to an increased ocean heat loss, and consequently a stronger outflow and a greater Atlantic heat transport. But a warm year increases the stratification due to ice melting and inhibits the mixing for creating the BSW. In contrast, a cold year favors cooling due to a large air-sea gradient temperature and winter ice production that releases a lot of salt making the water denser.

To summarize, a warming trend is identified in the BS highlighted by an unprecedented sea ice decline. This trend is accompanied by multi-annual oscillations both in the atmosphere circulation (AO) and ocean water mass characteristics.

1.3. Problematic: What could be the Impacts of this warming trend and long-term ocean-ice-atmosphere variability on the Barents Sea water masses distribution?

The water mass distribution is strongly constrained by the cyclonic global ocean circulation of the BS (**Fig.1b**) and the bottom topography (**Fig.1a**) especially in shallow areas. The Barents Sea Opening (BSO) is a shelf break where the eastward in-flowing water crosses over a 450m depth bathymetry at the maximum. The main inflow into the BS takes place through the BSO between Fugloya and Bjornoya and is constituted by the AW and the NCCW, which amount to about 2 Sv ([Ingvaldsen, Loeng et al. 2002](#)) and 1.1 Sv ([Skagseth 2008](#)) respectively. This shelf favors tides of high intensity especially in shallow and coastal areas like Svalbard for instance, which produces turbulent mixing. In order to investigate hydrological changes in the BS, it is necessary to study the structure as well as the seasonal and inter-annual variability of:

- 1) Water Masses distribution in a context of “Atlantification” pointed out by [Arthun et al \(2012\)](#) for the last decade. It is a process in the BS illustrated by an increase of the heat transport due to both an increase of the AW transport and temperature.

2) Barents Sea Polar frontal area. It is one of the major oceanographic feature in the BS ([Johannessen and Foster 1978](#); [Pfirman, Bauch et al. 1994](#); [Gawarkiewicz and Plueddemann 1995](#)). It delimitates the boundary between AW and ArW. It is associated with physical processes such as vertical mixing and cross frontal transport that are combined with the most vigorous ocean-air heat loss (~70TW just for BS) of the Arctic ([Serreze, Holland et al. 2007](#); [Smedsrud, Ingvaldsen et al. 2010](#)), which favors the winter BSW production. Despite this fact, only a few studies (e.g. [Parson, Bourke et al. 1996](#)) provided local description of a unique polar front in the western part of the BS. In contrast, no distinct frontal structure was ever mentioned in the Eastern BS so far ([Midttun and Loeng 1987](#)).

The BS water masses delimited by the BS polar front structure are of particular interest as the BS appears to play an important role in the Northern Hemisphere climate ([Smedsrud, Esau et al. 2013](#)) by ventilating the Arctic Ocean with the dense BSW ([Aagaard and Woodgate 2001](#); [Schauer, Loeng et al. 2002](#)) and by being a place of high primary productivity ([Loeng 1991](#)). But what do we know about the variability of the frontal structure and the water masses distribution in the BS? For the last 30 years, does the “Atlantification” mean an Arctic-ward extension of the Atlantic domain? What are the effects of this “Atlantification” on the frontal structure and on the BSW production?

1.4. Objectives

The BS is the only Arctic Sea with enough available in-situ observations to provide data covering the entire area and permitting reliable inter-annual summer variability analysis. A specificity of this study was to set up an extensive new dataset obtained from recent data collected by Russian in addition to the existing international data base. The use of the regional 3D SINMOD low (20km) and high (4km) resolution model outputs ([Slagstad and McClimans 2005](#)) will be used for completing the observations analysis especially for studying variability. The objective of this research is to investigate the temporal (seasonal and inter-annual) and spatial variability of the main water masses distribution and frontal structures all over the BS during the last 30 years (1980-2011).

2. DATA AND METHOD

2.1. A new extensive hydrographic data set collection

The BS is more likely the only Arctic region where presently in-situ observations are available and relevant for analyzing long-term ocean variability. Because it remains ice-free in summer and autumn, the BS is covered by standard hydrological sections characterized by a large number of vertical profiles. The International Council for the exploration of the Sea (ICES) and the Arctic and Antarctic Research institute (AARI, Russia) provided processed hydrographic data sets ([Nilsen et al., 2008](#)). ICES (<http://ocean.ices.dk>) and AARI ([Ivanov et al., 1996](#); [Korablev et al., 2007](#)) database is more likely the most complete hydrographic collection at present time for the BS.

The merged data base quality has a maximum resolution of 0.01 psu for salinity and 0.01°C for temperature. The accuracy of this data set is difficult to determine but the worst accuracy of the data might be as poor as 0.1°C and 0.1 psu. Although, the data set is better flagged than the NODC's one (<http://www.nodc.noaa.gov/OC5/SELECT/dbsearch/dbsearch.html>) and appears consistent when averaged appropriately. In order to have almost 100% of the BS surface covered by the data set, the study area has been limited to the box shown in **Fig.1a** (70-80°N 10°-65°E).

Within this domain, the data set contains more than 110 000 CTD profiles with some repeated sections like BSO (6 times a year, every two months) and KOLA (2 times a year, winter and summer). Note that there is less data in the Russian part of the BS during the last decade. However, this does not impact on the quality of the results. **Fig. 1c** presents the data coverage. It is situated at 100% in the Norwegian territory but this percentage decreases below 85% east of 45°E and reaches only 50%.

These observations are used to estimate the BSO temperature variability, the water mass characteristics and the mean state and variability of the polar frontal structure.

2.2. Krigging : an optimal method for interpolating data

Krigging is a technique that provides the Best Linear Unbiased Estimator of an unknown field (Journel and Huijbregts, 1978; Kitanidis, 1997). The originally sparsely sampled data are assumed to be statistically characterized by a semi-variogram which represents the spatial mean variability of the data. Its mean and standard deviation are independent of the position, but its co-variance function depends only on the distance between two data points. This co-variance function is used to derive a weighted average of the adjacent observations minimizing thus the variance estimation.

The temperature, salinity and density fields were interpolated for the summer period (August and September) horizontally onto a 0.5° longitude x 0.25° latitude grid and vertically for the KOLA section onto a 0.125° latitude x 5m depth grid. The horizontal fields were derived for the surface and for the averaged parameters within the layers 0-50m, 50-100m and 100-200m.

2.3. SINMOD 3-D Model Description and set-up (Slagstad, 1987)

SINMOD (SINtef Ocean MODel) is a coupled 3D hydrodynamic chemical and biological model system that has been developed and used for over 25 years at SINTEF (Scientist and Industrial Research Foundation, Norway). The hydrodynamic part of the model is based on the primitive equations which are solved by finite differences using an Arakawa C-grid ([Mesinger and Arakawa 1976](#)). The model uses z-coordinates in the vertical direction. The ice model is based on the elastic-viscous-plastic rheology described by Hunke and *Dukowicz (1997)*.

The model is forced by transports through open boundaries ([Slagstad and Wassmann 1996](#)), atmospheric fluxes, freshwater input and tides. The four tidal components (M2 , S2 , K1 and N2) were imposed by specifying the various components at the open boundaries of the large-

scale model. Data are taken from TPXO 6.2 (<http://www.coas.oregonstate.edu/research/po/research/tide/index.html>). Freshwater run-off, river discharge and run-off from land are based on outputs obtained from a simulation with a hydrological model (*Dankers and Middelkoop 2007*). The model was validated for the BS with in-situ current measurements and temperature fields, and was compared with physical and chemical observations provided from a section across the central part of the basin. The model was applied in an experimental setting forced by air-sea fluxes provided by the European Centre for Medium-Range Weather Forecasts (ECMWF) reanalysis data (ERAi). Initial values of temperature and salinity were taken from NODC World Ocean Atlas 1998 data (also known as the Levitus data base) provided by the NOAA-CIRES Climate Diagnostics Center, Boulder, Colorado, USA, on their Web site (<http://www.cdc.noaa.gov/>). For a more detailed model description, see *Slagstad et al. (1999)* and *Slagstad and McClimans (2005)*.

For this study, we used monthly temperature and salinity fields obtained from SINMOD runs performed for the 1979-2012 period over the whole Arctic with a 20km grid version with 25 levels and for the 1997-2001 period over the Nordic Seas with a 4km grid with 34 levels. Data were processed for computing water mass occurrences and indexes (cf next paragraph) at 100m as well as BSO temperatures in order to compare them with in-situ data.

The 4-km grid SINMOD outputs have been used for studying the frontal variability due to the need in accuracy for that specific study. The 20km resolution is too coarse to properly resolve fronts between water masses of different properties. Temperatures fields have been smoothed using a Gaussian spatial filter with a standard deviation of 36 km in order to get rid of meso-scale activity.

3. RESULTS AND DISCUSSION

3.1. Summer Climatology from observations

3.1.1. Water masses

3.1.1.1. Theta-S diagrams analysis & main water mass definitions

The following BS water mass characteristics are chosen for this study, based on BS water masses definitions adapted from literature (**table1**):

Atlantic Waters (AW): $S > 34.8$, $T > 3^{\circ}\text{C}$.

Arctic Waters (ArW): $S < 34.7$, $T < 0^{\circ}\text{C}$.

Barents Sea Waters (BSW): $S > 34.8$, $T \leq 2^{\circ}\text{C}$.

Norwegian Coastal Current Waters (NCCW): $S < 34.4$, $T > 3^{\circ}\text{C}$.

Then water types, which describe the ‘core properties’ of water masses, have to be accurately defined like single points in potential-temperature/salinity diagrams such as the black rectangles **Fig. 2** illustrating water mass definitions. Unambiguous criteria have been chosen for each water types. ArW is defined with a minimum of temperature because it is the coldest water mass and has an inflection in temperature between 34.2 and 34.4 psu (**Fig.2c**). BSW, as the densest BS water mass, is defined by a maximum of density. AW is the most saline water mass and the main source of salt in the BS (except brines but at colder temperature) and is thus defined by a maximum of salinity. NCCW is too variable in both temperature and salinity due to strong surface interactions (freshwaters inputs, solar heating...) and will not be defined as a water type.

For the 1980-1985 period, the Gimsoy transect in the Norwegian Sea (**Fig.1a**) allows to identify (**Fig.2a**) the summer AW (AW, 200m, 7°C, 35.25 psu), the intermediate Arctic Waters (IW) at 1200m correspond to 28.1 kg/m³, -1°C and 34,9 psu and the summer Norwegian Coastal Current Waters (NCCW, 0-100m, >6°C, <34.4 psu). The NCCW has a very large temperature and salinity seasonal variability. It can reach more than 12°C at surface in summer and range between 32 to 34.4 psu. For the same period, the area North of 80°N in the Nansen Basin is representative of the summer ArW (**Fig.2c**) (0-200m, T<0°C, S<34.7 psu). The three water masses (AW, NCCW, ArW) are the main water masses contributing to the BS water masses in general.

The summer AW, entering the BS at BSO is observable in **Fig.2b** and is different from the one in the Norwegian Sea. AW is modified by mixing between the Atlantic waters (AW) and the NCCW advected from the Norwegian Sea due to a high eddy activity especially between the Lofoten Basin (Gimsoy section) and BSO (**Fig.1**). Indeed, the AW receive a little amount of freshwaters in this area and its salinity decreased by more than 0.1 psu. Then, the AW is transformed by mixing with the ArW while flowing east toward KOLA section (**Fig.2d**). Mixing between AW and ArW is represented **Fig.2** by a dashed line. Note that cooling and freshening of AW is favored along BSO (**Fig.2b**) and KOLA (**Fig.2d**) by water column homogenization and mixing during winter. AW seasonal variations at BSO or KOLA are smaller than 1°C in temperature and 0.1 psu in salinity. No significant seasonal variability is found for BSW at depth.

All these water masses have large differences both in salinity and temperature. The mixing and cooling between AW and ArW will produce the so-called « Barents Sea Atlantic derived water », also denoted « modified Atlantic Water » or « Polar Front Waters ». The BSW is represented **Fig.2b** and **Fig.2d**. These dense waters (>27.8 kg/m³ and 28.1 kg/m³ for the densest ones) are formed on the BS shallow banks (mainly the Central Bank) and then cascade down the deeper regions ([Årthun, Ingvaldsen et al. 2011](#)) to finally flow out the BS toward the Arctic Ocean to form the Intermediate Arctic Waters ([Rudels, Jones et al. 1994](#)). In **Fig.2c**, the BSW, as expected, are formed by a mixing between the ArW and AW and large heat losses (temperature decreased from 6°C of to 0°C for the densest BSW formed in winter). It is in agreement with BSO AW temperature around 6°C measured by ([Årthun and Schrum 2010](#)) compared to the temperature of the section between Nova Zemlya and Franz

Josef Land around 0°C ([Gammelsrød, Leikvin et al. 2009](#)). The densest BSW (-1,5°C, 34,9 psu, not shown) found East of KOLA section have quite the same hydrographic properties than intermediate waters at 1200m depth in the Arctic Ocean (**Fig.2a & Fig.2c**). This validates the fact that local shelf convection forms the Arctic Intermediate Waters.

3.1.1.2. Water mass occurrences

The temperature-salinity analysis consists in distinguishing water masses in order to derive water mass occurrences given in percentage for the 1980-2011 period. The water mass occurrences were derived within the 50-100m layer from hydrographic gridded data. The choice of this layer depth will be explained further in the paragraph 3.1.2.1. The summer water mass occurrences in percentage vary from 0 to 100%. An occurrence of 100% means that the water mass is always present each year during the 1980-2011 summer period. The water mass index is computed every year as the number of grid points for which the concerned water mass is detected divided by the total number of grid points of the map. It reflects the relative volume occupied by each of the water masses in the studied area.

Fig.3a shows that AW is present in the South-west BS, in the BSO trough and up to the Great Bank, with an occurrence equal to 100%. The AW sometimes spreads further north and east in the deepest part of the BS (occurrence approximately equal to 20-30% in these areas). The ArW occurrence (**Fig.3b**) is close to 100% in the North-West BS and over the Spitsbergen bank. The locally formed BSW (**Fig.3c**) mainly resides in the Central Bank as expected ([Årthun, Ingvaldsen et al. 2011](#)). The NCCW (**Fig.3d**) has a significant contribution in the southern part of the BS as it accounts for about one third of the inflowing waters through BSO. NCCW are maintained near the coast west of 30°E by the Norwegian coastal current, and then they spread up to 74°N with the addition of surface fresh waters from the White Sea, Pechora Sea, Kara Sea and rivers.

In general, the eastern BS is less dynamically constrained by topography ([Parson, Bourke et al. 1996](#)). The water masses structures are more diffuse with water mass occurrences lower than 30% and they do not strictly follow the isobaths. As an example, no water mass is dominating east of 40°E. Observations confirm that coastal shallow area (<200m) of the Eastern BS is influenced by the four main water masses, i.e. AW, ArW, BSW and NCCW. There is also a large contribution of ice in the surface fresh layer (not shown). The BSW is deeper than the AW and the ArW because its density is higher. An extra water mass, the Spitsbergen Bank water mass, is not considered in this study. This is why AW is observed at the same place as ArW on the Spitsbergen bank (**Fig.3a & 3b**) which is not realistic. The Spitsbergen Bank water mass is formed from the mixing of fresh melt waters from Spitsbergen glaciers and ice with the AW carried out by recirculating currents. However **Fig.3a** reveals an AW occurrence at these locations lower than 20%. As a conclusion, water masses are well separated in the Western BS where the barotropic flows are trapped by large gradients of bathymetry ([Johannessen and Foster 1978](#); [Gawarkiewicz and Plueddemann 1995](#)) and they are overlapping in the Eastern BS where the control of the bathymetry is less important because it is flatter.

3.1.2. Description of the polar front structure

3.1.2.1. Vertical description of the polar front structure along the KOLA section

The KOLA section (at ~31.5°E) is situated at a critical place in the BS (**Fig.1a**). Indeed, the ocean bottom topography is smoother east of KOLA section (**Fig.1a**) and ArW and AW cease to be in contact directly (**Fig.3a & b**). KOLA section has been kriggered with temperature (**Fig.4a**) and salinity (**Fig.4b**) and averaged over the 1980-2011 period during September.

The core of the ArW ($T < 0^{\circ}\text{C}$) is observed **Fig.4a** in subsurface over the Great Bank. The AW ($T > 3^{\circ}\text{C}$, $S > 34.7$) remains in the middle-south of the section between 0 and 60 m while the BSW (density $> 1027.8 \text{ kg/m}^3$) underlies the ArW and AW over the central bank resulting in a “doming” of the density structure. The NCCW ($S < 34.4$) core is also clearly appearing in the surface layer of the southern BS, resulting in AW deeper than 50m south of the SPF. The mixed layer depth (density $< 1027.4 \text{ kg/m}^3$) is modulated by horizontal temperature gradient south of the SPF following the 6°C isotherms. It reaches about the same depth (30m) in the north BS but due to salinity gradients.

We will avoid the surface layer in summer because of its very large variance in temperature ($1\text{-}3^{\circ}\text{C}$, **Fig.12c annex**) and salinity (0.2-0.8 psu, **Fig.11c annex**). Furthermore, gradients are more accurate in sub-surface within the 50-100m layer even if they are weaker. The pattern of frontal structures is also better defined at depths deeper than 50m avoiding the surface layer influenced by the strong summer atmosphere-ocean heat exchanges. These sub-surface layers better catch the AW inflow especially in the Eastern BS where freshwater from Pechora and White Seas and ice melting could biased the frontal structure pattern at surface. Even if ice could be a good indicator for ArW, we cannot so far relate melt waters with polar front and the ArW. Layers deeper than 100m are also avoided because the frontal structure is more diffuse (i.e. weaker gradients) attributed to vertical mixing due to shear turbulence related to the tidal flow ([Parson, Bourke et al. 1996](#)).

A front is delimiting two water masses and physically corresponds to a maximum of the temperature and/or salinity gradient. Dynamically speaking, a front is a maximum in density gradient dominated either by temperature, salinity or both. Temperature and salinity can also compensate in density and temperature and salinity fronts do not necessarily correspond to a density front. Four horizontal gradients are illustrated **Fig.4c** with vertical lines. They can be observed in the horizontal temperature and salinity gradient **Fig.11b & 12b** (annex). Density Ratio D_x is a measure of the relative effect of temperature and salinity on the horizontal density gradient in the front, a dimensionless horizontal density ratio was computed based on [Rudnick and Ferrari \(1999\)](#) relationship:

$$D_x = \alpha \cdot \theta_x / \beta \cdot S_x$$

Where α is the thermal expansion coefficient for seawater, β is the haline contraction coefficient, θ_x and S_x are horizontal potential temperature and salinity gradients in $^{\circ}\text{C}/\text{m}$ and psu/m. Density ratio (D_x) in **Fig.8** (annex) indicates that two of the four gradients are

dominated by temperature ($D_x > 1$) and two by salinity ($D_x < 1$) respectively in red and blue **Fig.4c**.

The first front at 71.5°N , which is essentially the position of the Norwegian Coastal Current, is a density front (**Fig.12b**, annex) dominated by a large salinity gradient >0.01 psu/km (**Fig.10b**, annex) and a density ratio $0 < D_x < 1$ (**Fig.13 annex**). This front, the Norwegian Coastal Current Front (NCCF), is separating the fresh CW from the saline AW and is collocated with the 34.8 isohaline (**Fig.4b**). Then, a weak front dominated by temperature (**Fig.11b & 13**, annex, $>0.04^\circ\text{C}/\text{km}$, $D_x > 1$) is found at 74°N on the Central bank slope associated with the 4°C isotherm (**Fig.4a**). The Kola section, which passes over the Central Bank, is crossing the path of BSW (**Fig.3c**) and consequently generating a small temperature gradient between the warm AW and the colder BSW. This front is a meander of the South polar front (SPF). Between 76.2°N and 77.2°N , a strong frontal zone dominated by temperature gradient (**Fig.11b & 13**, annex, $>0.2^\circ\text{C}/\text{km}$, $D_x > 1$) is observed in between the 2°C and -0.5°C isotherms (**Fig.4a & c**). The southern boundary of this frontal zone is in agreement with the 2°C isoline (**Fig.4a**) as noticed by *Parson et al.* ([1996](#)) and follows roughly the 200m isobath south of the Great Bank (**Fig. 4c**) which is not far from the 250m isobaths estimated by *Harris et al.* ([1998](#)). Finally, at 77.2°N , a last front dominated by large salinity gradients (**Fig.10b & 13**, annex, >0.01 psu/km, $D_x < 1$) is observed at the same place as the 34.6 isohaline and more approximately as the -0.5°C isotherm (**Fig.4**).

To summarize, three fronts are detected. From south to North, we note the Norwegian Coastal Current Front at 71.5°N , the South Polar Front (SPF) at 74°N and 76.2°N , and the North Polar Front (NPF) at 77.2°N . Hydrography does not therefore indicate a unique polar front, but two offshore fronts in addition to the Norwegian coastal current front. The dense waters in **Fig.4** (> 1027.8 kg/m³) are located exactly in between the SPF at 74°N and the NPF at 77.2°N within the 50-100m layers over the shelf breaks of the Great and Central Banks. The NPF is sharply identified by salinity gradients whereas temperature gradients are indicating a frontal zone where the SPF and NPF are respectively the southern and the northern boundaries.

3.1.2.2. *Subsurface description of the 2D polar front structure.*

In order to identify fronts on horizontal maps, probability density functions (PDF) of temperature and salinity, associated with norm of gradients larger than $0.1^\circ\text{C}/\text{km}$ and 0.01 psu/km respectively, were derived (**Fig.5a & b**). For that, we computed the west-east and north-south gradient components and then calculated the norm of the gradient. Thus, only large gradients likely to belong to the frontal structures were selected. Gaussian-like distributions were computed. Peaks in the Gaussian distributions indicate the most frequent temperature or salinity values collocated with large gradients in the dataset. Those values were chosen as the corresponding isolines of the front. In case where no significant peak was detected due to a too smoothed distribution (excess kurtosis ≤ 0), the frontal zone is described by a standard deviation bandwidth where the maximum density of large gradients might be found.

Mean density fields within the 50-100m layer derived from hydrographic krigged data are shown in **Fig.6a** (summer temperature climatology) & **6b** (summer salinity climatology). The NPF, (in solid blue line in **Fig.6b**), is defined by the 34.6 isohaline in agreement with the KOLA section presented in **Fig.4c**. The PDF of the gradient salinity fields (**Fig.5a**) shows a normal gaussian distribution (excess kurtosis = 0) with a negative skewness. The PDF of the temperature gradient fields (**Fig.5b**) which has a negative excess kurtosis (and a positive skewness) illustrates the fact that the temperature does not describe a front line but a frontal zone. The SPF, which is characterized by the southern boundary of the temperature frontal zone, is defined by the 2°C isotherm in red solid lines in **Fig.6a** and has quite the same pattern than the front represented by *Harris et al. (1998)*.

The mean temperature gradients diminishes from 0.2°C/km in the West to less than 0,05°C/km in the East of the BS (**Fig.14b**, annex) and the salinity gradient from 0.02 psu/km to less than 0.004 psu/km respectively (**Fig.15b**, annex). The existence of the NPF in the North-east is questionable regarding the temperature and salinity gradients whereas the SPF is still detectable, even if the gradients are weaker. The largest temperature temporal variability up to 2°C (**Fig.15c**, annex) between the -0.3°C and 2°C isotherms corresponds to the frontal zone. The salinity has large variability up to 0.04 psu near the coasts of Norway, Svalbard and Novaya Zemlya as well as along the NPF (**Fig.14c**, annex).

As observed for the KOLA section (**Fig.4**), the SPF and the NPF split in two branches. One branch appears between Svalbard, the Bear Island and up to the Great Bank where the AW and ArW are directly in contact and creating strong gradients. But further east, two branches appear (ie SPF & NPF) with a mixing frontal zone in between, with large temperature variability. This is where the BSW are generated. The BS fronts are highly constraint by bank areas. The SPF is roughly following the 200m isobath and NPF the 150m isobath.

3.2. Water Mass Variability in the atmosphere-ice-sea system context

3.2.1. From Observations

3.2.1.1. Changes in water types properties from Theta-S Diagram analysis: toward warmer and more saline AW

Warmer and saltier incoming AW coming from the Norwegian Sea are observed comparing 2005-2010 (**Fig.7a**) and 1980-1985 (**Fig.2a**) periods. The summer surface AW at Gimsoy section (triangle in **Fig.2a**) experiences an increase of about +1 °C in temperature and +0.05 psu in salinity during the last thirty years (1980-2010) illustrated by a black arrow **Fig.7a**. This increase of temperature and salinity is also observed in the BS in BSO and KOLA sections with +0.2°C/+0.05psu (**Fig.7b**) and +1°C/+0.02psu (**Fig.7c**) respectively. BSW also experience modifications at depth. BSW temperature and salinity increase by +1.5°C/+0.1psu at BSO and 0.8°C/0.02 psu at KOLA respectively. Arctic Waters in circle have remained remarkably steady across time (not shown). These results confirm that the warming observed in the BS for AW and even for BSW at depth is partly due to warmer AW advected from the Norwegian Sea where the Gimsoy section is situated. The AW seasonal variability didn't

significantly change between 1980-1985 and 2005-2010 at BSO and KOLA sections (winter AW in empty triangle in **Fig.7b & c**).

3.2.1.2. *Water Mass Indexes: the “Atlantification” regime*

The water mass indexes indicate an increasing trend of AW index in the BS and a decrease of ArW over the last 30 years (**Fig.8e**). AW index is twice larger in 2011 (0.4) than in 1980 (0.2). This “Atlantification” is in agreement with *Årthun et al. (2011)* which coincides with a large reduction of Sea Ice (-200000 km² at least **Fig.8b**). The increasing trend of about +1°C and +0.2 psu found at BSO section between 50 and 200m (**Fig.8g & h**) is similar to the one observed previously in the Theta-S diagrams between 1980-1985 and 2005-2010 at Gimsoy section (ie +1°C and +0.05 psu, **Fig.3a & b**). This “Atlantification” comes along with a warmer (and saltier) BS partly due to warmer (and saltier) incoming AW.

An oscillation between cold and warm events is observed in relation with the sea ice extent (**Fig.8b**) which is a good indicator for the BS climate environment (*Serreze, Barrett et al. 2006*). This 5-7 year period oscillation in ice cover variation, in agreement with *Furevik (2001)*, is linked to the oceanic forcing (ie AW inflow against ArW in the BS) but also with atmospheric conditions (AO, SAT, Heat loss). The extreme warm events (1983-1984, 1990-1991, 2000, and 2007) are clearly related to a high AW index and a low ArW index (**Fig.8e**). Cold events in bright blue vertical lines (1981-1982, 1987-1988, 1994, 1998, 2003-2004 and 2010) usually appear after high ArW index and low AW index. They are happening during low/negative AO index (**Fig.8a**) which suggests an amplified cyclonic atmospheric circulation. In the same way, a cold event is related to a cold atmospheric temperature associated with a strong ocean-atmosphere temperature gradient which may favor heat loss to the atmosphere (**Fig.8c & d**).

3.2.2. *From model*

The BSW are mainly formed in winter and the hydrographical observations mainly described the summer situations. Water masses index derived from the 100m layer of SINMOD outputs complete the observations for the seasonal and interannual variability analysis.

Fig. 8f and **Fig.8g** show that the model with a 20km resolution overestimates the temperature by about 1°C for the first 12 years between 1980 and 1992 and underestimate salinity by about -0.1 psu (especially during recent years). From 1993 to 2011, model temperatures are similar to in-situ observations. When the resolution increases to 4km (from 1997 to 2001), the model overestimates the temperature by +0.8°C and underestimate the salinity by -0.1 psu. These biases have to be kept in mind for further analysis since they correspond to a global underestimation of about 0.1kg/m³ in density. This might be due to the fact that the model is producing deeper mixed layer than those observed and over-homogenized deep water (*Sundfjord, Fer et al. 2007; Ellingsen, Slagstad et al. 2009*). The model cannot reproduce the trend observed in the observations in agreement with *Ellingsen et al. (2009)* due to a lack of an important forcing. For example, the BSO temperatures of the SINMOD 20KM oscillate between 5 and 6°C whereas according to observations, it should vary from 4 to 6°C (**Fig.8g**).

However, the inter-annual variability is successfully described and confirmed by the model with correlations between observation and model of about 0.7 in temperature.

The water masses indexes from SINMOD reveal the seasonality as well as the interannual variability of the water masses (**Fig.8f**). The seasonality variability confirms that BSW is produced in winter (February-March) while the ArW index and ice production are maximum. The AW contribution is maximum during autumn (October-November) and NCCW during November-December. On an interannual scale, the “Atlantification” trend is not observed in the model. The BSW index also appears to be largely under-estimated whereas NCCW are over-estimated due to low model densities related to warmer and fresher waters than in the observations.

Besides, a very interesting result is that the BSW production (**Fig.8f**) generally increases just before a cold event. Before a cold event, the cooling from the ocean is the most effective with differences between air and sea surface temperature larger than 15°C (**Fig.8c**), a salinity remains larger than 34.9 psu (**Fig.8f**) due to a still large AW index, weak NCCW contribution (**Fig.8h**) and huge winter heat loss to the atmosphere (from -200 to -300 W/m², **Fig.8d**).

3.3. Variability of the fronts (SPF & NPF) : a model study

In 1998 and 2000, which were respectively cold and warm years, drastic changes were observed over the BS. Within this short period, the BS experienced a shift from an AO⁺ to an AO⁻ which comes along with a decrease of about 200,000 km² of the winter sea ice extent, an increase of about +1°C in the BSO temperature, +10°C in winter of the atmosphere temperature at 2m and +0.5°C in the winter SST (**Fig. 8a, b & c**). It shows a shift toward a relative AW domination in the BS. From observations (**Fig.8e**), the AW index increases from 0.4 to 0.5 and the ArW remained steady whereas in the model (**Fig.8f**), the ArW index decreases from 0.4 to 0.3 while the AW index increased from 0.25 to 0.35. As the model does not reproduce the trends, comparison of SPF and NPF between a cold and a warm event such as those occurring in 1998 and 2000, might suggest how BS would behave if “Atlantification” continues for a longer time.

During the 1998 winter, the SPF (**Fig.9a**) was collocated with the 1.4°C isotherm. The isotherms corresponding to the SPF are changing and getting warmer. 3.9°C during summer 1998, 2.2°C during winter 2000, and 4.6°C during summer 2000 (**Fig.16**, annex). These temperatures from SINMOD are +2.25°C warmer than the hydrography measurements (2°C in summer) but in agreement with an over-estimation of model temperature by more than 1°C. We assume this is a systematic bias of the model between 1997 and 2001. The NPF corresponds to the 34.7 isohaline in winter and summer 1998, 34.84 isohaline in winter and winter 2000 (**Fig.18**, annex). Salinity is then quite over estimated (+0.1/+0.24 psu) by the model compared with hydrography (34.6 psu).

3.3.1. *Comparison between two contrasted years: the cold 1998 and the “Atlantified” 2000.*

The SPF isotherms shift by about $+0.8^{\circ}\text{C}$ from 1998 to 2000. This might be due to larger contribution of AW through the BSO and a decrease in freshwaters inputs from the Sea ice melting during summer in 2000. The NPF isohalines shift by about $+0.14$ psu in winter and summer. Most of the changes into the SPF and NPF inter-annual variations are taking place in the eastern part of the BS (**Fig.9a & b**). For example, NPF have stronger gradients in the North-East BS in 2000 (**Fig.18**, annex). The eastern part of the SPF is moving northward and eastward. Indeed, since it is less topographically constrained than in the west, SPF can propagate northward into the Central Basin between the 200 m and 300 m isobaths. It then creates new salinity and temperature gradients all around Novaya Zemlya Bank in the Eastern BS (>0.08 $^{\circ}\text{C}/\text{km}$ and >0.008 psu/km) such as those observed during a warm year in which the dominating front in the east BS shifts from the SPF to the NPF, at least as far as temperature gradient (**Fig.16**, annex) are concerned.

3.3.2. *Seasonality*

From winter to summer, in 1998 and 2000, the isotherms defining the SPF are shifting by $+2.4^{\circ}\text{C}$ (from 1.4°C and 2.2°C respectively) whereas isohalines for NPF isohalines remain the same (34.7 and 34.85 respectively). The SPF and NPF have quite similar patterns between summer and winter (**Fig.9a & b**). Constrained by the bathymetry of the Great Bank, the Central Bank, the Novaya Zemlya Bank and the Pechora Sea shelf, the ongoing eastward AW flow progresses further North and East into the Eastern BS. Both fronts are trapped between the 150 m and 250m isobaths and are experiencing an intensification of all gradients during summer. The NPF is the strongest temperature and salinity front during winter (**Fig.17 & 19**, annex) and the salinity gradients increases from 0.006 to more than 0.015 psu/km. The SPF intensifies during summer especially in the South over the Central Bank and the Central Basin from 0.05-0.06 $^{\circ}\text{C}/\text{km}$ to more than 0.1 $^{\circ}\text{C}/\text{km}$. The seasonal variations of SPF and NPF are well marked in term of gradient intensity rather than in geographical position.

4. CONCLUSION

Hydrographic observations highlighted a significant “Atlantification” of the Barents Sea (BS) during the last 30 years. A saltier and warmer incoming Atlantic Water (AW) was observed from the Norwegian Sea through the Barents Sea opening (BSO). This especially affected the Eastern BS at the expense of the Arctic Waters (ArW). The trend has been amplified for the last decade and accompanied by the largest Sea ice decrease in the BS ever observed during the last 30 years.

The “Atlantification” led us to investigate the BS variability of the frontal structure. The polar front structure was composed of a unique branch in the West, but splitted into two well identified structures in the East part where gradients are weaker due to a reduced bottom topography roughness. The Barents Sea Waters (BSW) was formed in between these two

fronts: The South Polar Front (SPF) was dominated by temperature and collocated with the 2°C isotherm and the North Polar Front (NPF) was dominated by salinity collocated with the 34.6 isohaline.

BSW and polar fronts was dependent on a 5-7 years oscillation of the Ocean-ice-atmosphere system which modulated the “Atlantification” trend of the BS. This oscillation has been defined with Sea ice as an indicator of the system but is present in the atmosphere (surface air temperature) as well as in the Ocean (Water mass indexes, SST, BSO temperature). The Arctic Oscillation index period is hard to define on such a short time scale but negative AO index, when related to cold events, provides favorable conditions for BSW production whereas a positive AO index amplifies the “Atlantification”. However, the Arctic Oscillation index does not appear as a fully adapted indicator of the atmospheric long-term variability of the Barents Sea.

The front variability study shows a substantial northward shift of the eastern part of the SPF along the 200-300m isobaths between the cold 1998 (negative AO index) and the warm “Atlantified” 2000 (positive AO index) years despite bathymetric control whereas the NPF remains stationary. The BSW have been affected by the reduction of the formation area and by the decrease of the ArW. During the last decade, which is the warmest observed period, production of dense BSW was almost absent in winter in the SINMOD model. This suggests that if “Atlantification” increases, winter cooling and mixing with ArW will not be sufficient to produce dense BSW anymore and thus will impact on the Arctic Ocean ventilation. This might be attributed to a decrease of the ocean-atmosphere temperature gradient (heat loss), winter sea ice production and to an increased freshwater contribution from NCCW.

The BS can be considered as a robust ocean cooler and acts like a buffer zone between the global ocean and the Arctic. But at a time of drastic climate change, the ocean-atmosphere-ice system of the BS suffers important modifications. The Eastern BS is the most affected region due to the arctic-ward shift of the APF and seems to be no longer able to produce large amounts of dense waters anymore. Those physical changes might have significant impacts on phytoplankton and thus on the fisheries in the BS, which amount to an income up to 11.6 billions of euros for Norway economy.

The use of the high resolution SINMOD model outputs reinforced the observations in this study. The model at BSO under-estimated the density by about 0.1-0.2 kg/m³ in comparison with observations. The SINMOD model also did not succeed in representing the trend in temperature and salinity at BSO (Note however that BSO is not a good proxy for the entire Barents Sea ([Ingvaldsen, Loeng et al. 2003](#))). Hydrographic observations and the SINMOD model successfully described and confirmed that the inter-annual 5-7 year oscillation between cold and warm events found by [Furevik et al. \(2001\)](#) for the 1981-1996 period is still applicable for a longer period (up to 2011).

Glossary of Acronyms

AO: Arctic Oscillation index

AW: Atlantic Waters

ArW: Arctic Waters

BS: Barents Sea

BSO: Barents Sea Opening (BS AW entrance section)

BSW: Barents Sea Waters

IW: Intermediate Arctic Waters

NCCF: Norwegian Coastal Current Front

NCCW: Norwegian Coastal Current Waters

NPF: North Polar Front

SPF: South Polar Front

5. BIBLIOGRAPHY

Aagaard, K. and R. A. Woodgate (2001). "Some thoughts on the freezing and melting of sea ice and their effects on the ocean." Ocean Modelling **3**: 127-135.

Anderson, L. G., E. P. Jones, et al. (1999). "Ventilation of the Arctic Ocean estimated by a plume entrainment model constrained by CFCs." Journal of Geophysical Research **104**(C6): 13423.

Årthun, M., T. Eldevik, et al. (2012). "Quantifying the Influence of Atlantic Heat on Barents Sea Ice Variability and Retreat*." Journal of Climate **25**(13): 4736-4743.

Årthun, M., R. B. Ingvaldsen, et al. (2011). "Dense water formation and circulation in the Barents Sea." Deep Sea Research Part I: Oceanographic Research Papers **58**(8): 801-817.

Årthun, M. and C. Schrum (2010). "Ocean surface heat flux variability in the Barents Sea." Journal of Marine Systems **83**(1-2): 88-98.

Dankers, R. and H. Middelkoop (2007). "River discharge and freshwater runoff to the Barents Sea under present and future climate conditions." Climatic Change **87**(1-2): 131-153.

Ellingsen, I., D. Slagstad, et al. (2009). "Modification of water masses in the Barents Sea and its coupling to ice dynamics: a model study." Ocean Dynamics **59**(6): 1095-1108.

Furevik, T. (2001). "Annual and interannual variability of Atlantic Water temperatures in the Norwegian and Barents Seas:1980-1996." Deep-Sea Research **I**(48): 383-404.

Gammelsrød, T., Ø. Leikvin, et al. (2009). "Mass and heat transports in the NE Barents Sea: Observations and models." Journal of Marine Systems **75**(1-2): 56-69.

- Gawarkiewicz, G. G. and A. J. Plueddemann (1995). "Topographic control of thermohaline frontal structure in the Barents Sea Polar Front on the south flank of Spitsbergen Bank." Journal of Geophysical Research **100**(C3): 4509-4524.
- Harris, C. L., A. J. Plueddemann, et al. (1998). "Water mass distribution and polar front structure in the western Barents Sea." Journal of Geophysical Research **103**(C2): 2905.
- Hunke, E. C. and J. K. Dukowicz (1997). "An Elastic–Viscous–Plastic Model for Sea Ice Dynamics." Journal of Physical Oceanography **27**(1849-1867).
- Ingvaldsen, R., H. Loeng, et al. (2002). "Variability in the Atlantic inflow to the Barents Sea based on a one-year time series from moored current meters." Continental Shelf Research **22**: 505–519.
- Ingvaldsen, R., H. Loeng, et al. (2003). "Climate variability in the Barents Sea during the 20th century with focus on the 1990s." ICES Marine Science Symposium(Edinburgh).
- Ingvaldsen, R. B. (2004). "Velocity field of the western entrance to the Barents Sea." Journal of Geophysical Research **109**(C3).
- Inoue, J., M. E. Hori, et al. (2012). "The Role of Barents Sea Ice in the Wintertime Cyclone Track and Emergence of a Warm-Arctic Cold-Siberian Anomaly." Journal of Climate **25**(7): 2561-2568.
- Johannessen, O. M. and L. A. Foster (1978). "A note on the topographically controlled Oceanic Polar Front in the Barents Sea." Journal of Geophysical Research **83**(C9): 4567.
- Loeng, H. (1991). "Features of the physical oceanographic conditions of the Barents Sea." Polar Research **10**(1): 5-18 in Sakshaug, E., Hopkins, C. C. E. & Britsland, N.A. (eds.): Proceedings of the Pro Mare Symposium on Polar Marine Ecology.
- Martin, S. and D. J. Cavalieri (1989). "Contributions of the Siberian shelf polynyas to the Arctic Ocean intermediate and deep water." Journal of Geophysical Research **94**(C9): 12725.
- Mesinger, F. and A. Arakawa (1976). "Numerical methods used in atmospheric models." Global Atmospheric research programme - WMO-ICSU joint organizing committee **1**(17).
- Midttun, L. and H. Loeng (1987). "Climatic variations in the Barents Sea." the effect of oceanographic conditions on distribution and population dynamic of commercial fish stocks in the Barents Sea - proceeding of the third Soviet-Norwegian Symposium, Murmansk, 26-28 May 1986.
- Parson, A. R., R. H. Bourke, et al. (1996). "The Barents Sea Polar Front in summer." Journal of Geophysical Research **101**(C6): 14,201-214,221.
- Pfirman, S. L., D. Bauch, et al. (1994). "The Northern Barents Sea : Water Mass Distribution and Modification." Geophysical Monograph **85**(The Polar Oceans and Their Role in Shaping the Global Environment).
- Proshutinsky, A. Y. and M. A. Johnson (1997). "Two circulation regimes of the wind-driven Arctic Ocean." Journal of Geophysical Research **102**(C6): 12493.
-

- Rudels, B., E. P. Jones, et al. (1994). "On the Intermediate Depth Waters of the Arctic Ocean." Geophysical Monograph **85**(The Polar Oceans and Their Role in Shaping the Global Environment).
- Rudnick, D. L. and R. Ferrari (1999). "Compensation of Horizontal Temperature and Salinity Gradients in the Ocean Mixed Layer." Science **283**: 526-529.
- Schauer, U., H. Loeng, et al. (2002). "Atlantic Water flow through the Barents and Kara Seas." Deep-Sea Research I(49): 2281–2298.
- Schauer, U., R. D. Muench, et al. (1997). "Impact of eastern Arctic shelf waters on the Nansen Basin intermediate layers." Journal of Geophysical Research **102**(C2): 3371.
- Screen, J. A. and I. Simmonds (2010). "The central role of diminishing sea ice in recent Arctic temperature amplification." Nature **464**(7293): 1334-1337.
- Serreze, M. C., A. P. Barrett, et al. (2006). "The large-scale freshwater cycle of the Arctic." Journal of Geophysical Research **111**(C11).
- Serreze, M. C., M. M. Holland, et al. (2007). "Perspectives on the Arctic's Shrinking Sea-Ice Cover." Science **315**(5818): 1533-1536.
- Skagseth, Ø. (2008). "Recirculation of Atlantic Water in the western Barents Sea." Geophysical Research Letters **35**(11).
- Slagstad, D., K. Downing, et al. (1999). "Modelling the carbon export and air-sea flux of CO₂ in the Greenland Sea." Deep-Sea Research II **46**: 1511-1530.
- Slagstad, D. and T. A. McClimans (2005). "Modeling the ecosystem dynamics of the Barents sea including the marginal ice zone: I. Physical and chemical oceanography." Journal of Marine Systems **58**(1-2): 1-18.
- Slagstad, D. and P. Wassmann (1996). "Climate Change and carbon flux in the Barents Sea: 3-D simulations of ice-distribution, primary production and vertical export of particulate organic carbon." National Institute of Polar Research(51): 119-141.
- Smedsrud, L. H., I. Esau, et al. (2013). "The Role of the Barents Sea in the Arctic Climate System." Reviews of Geophysics **51**(3): 415-449.
- Smedsrud, L. H., R. Ingvaldsen, et al. (2010). "Heat in the Barents Sea: transport, storage, and surface fluxes." Ocean Science **6**: 219–234.
- Sundfjord, A., I. Fer, et al. (2007). "Observations of turbulent mixing and hydrography in the marginal ice zone of the Barents Sea." Journal of Geophysical Research **112**(C5).
- Thompson, D. W. J. and J. M. Wallace (1998). "The Arctic oscillation signature in the wintertime geopotential height and temperature fields." Geophysical Research Letters **25**(9): 1297-1300.



FIGURES

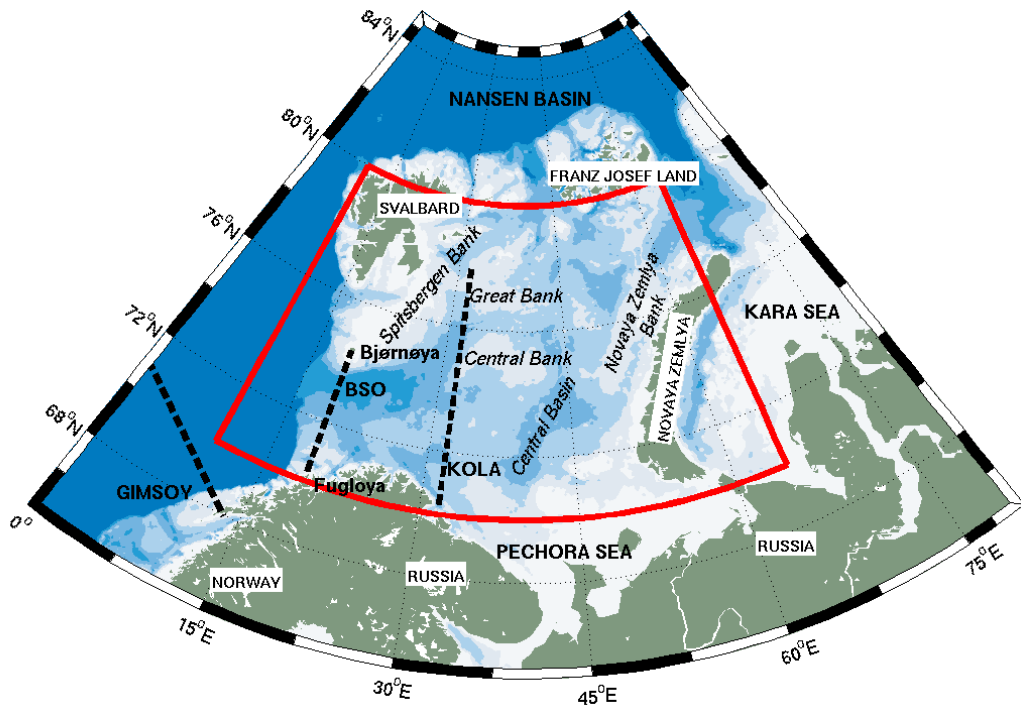


Figure 1a: Barents Sea map with bathymetry. 50m, 100m, 200m, 300m, 400m, 500m, 600m, and 700m isobath contours are plotted. The red line delimits the studied area. Repeated sections are represented in dashed black line: GIMSOY, BSO (Barents Sea Opening) and KOLA.

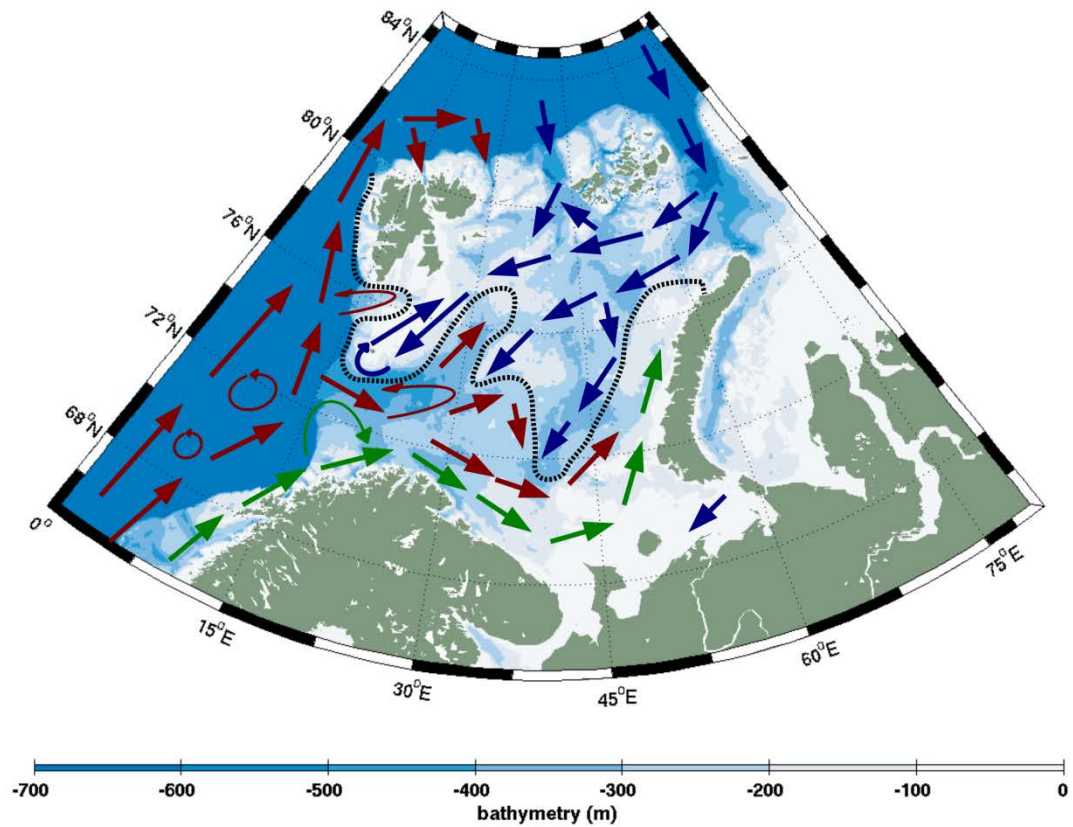


Figure 1b: Schematic surface circulation of main water masses (Atlantic water: red arrows ; Arctic water: blue arrows ; Norwegian Coastal Current : green arrows) and approximated location of the oceanic polar front in dashed line (adapted from Harris et al., 1998).

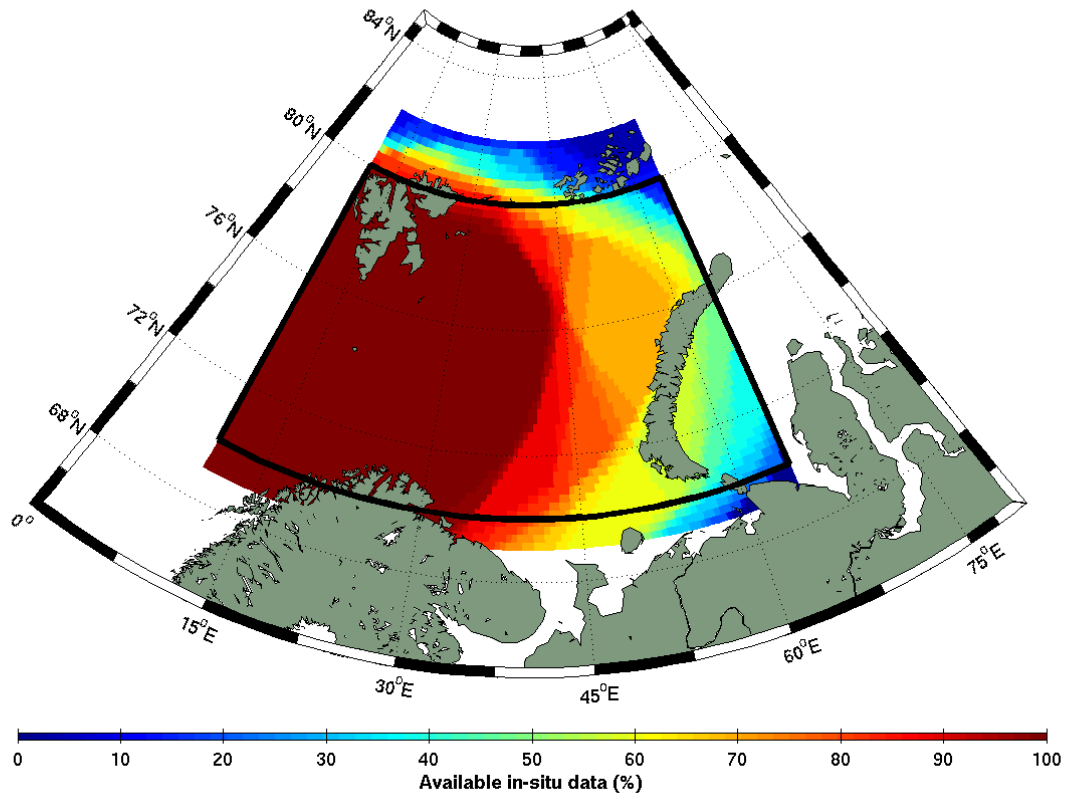


Figure 1c: Available in-situ data. 100 % data coverage at a grid mesh (0,5°C x 0,25°C) indicates there is a station for each summer (august-september) during the 1980-2011 period. The lowest in-situ data coverage in the Barents Sea is around 50%.

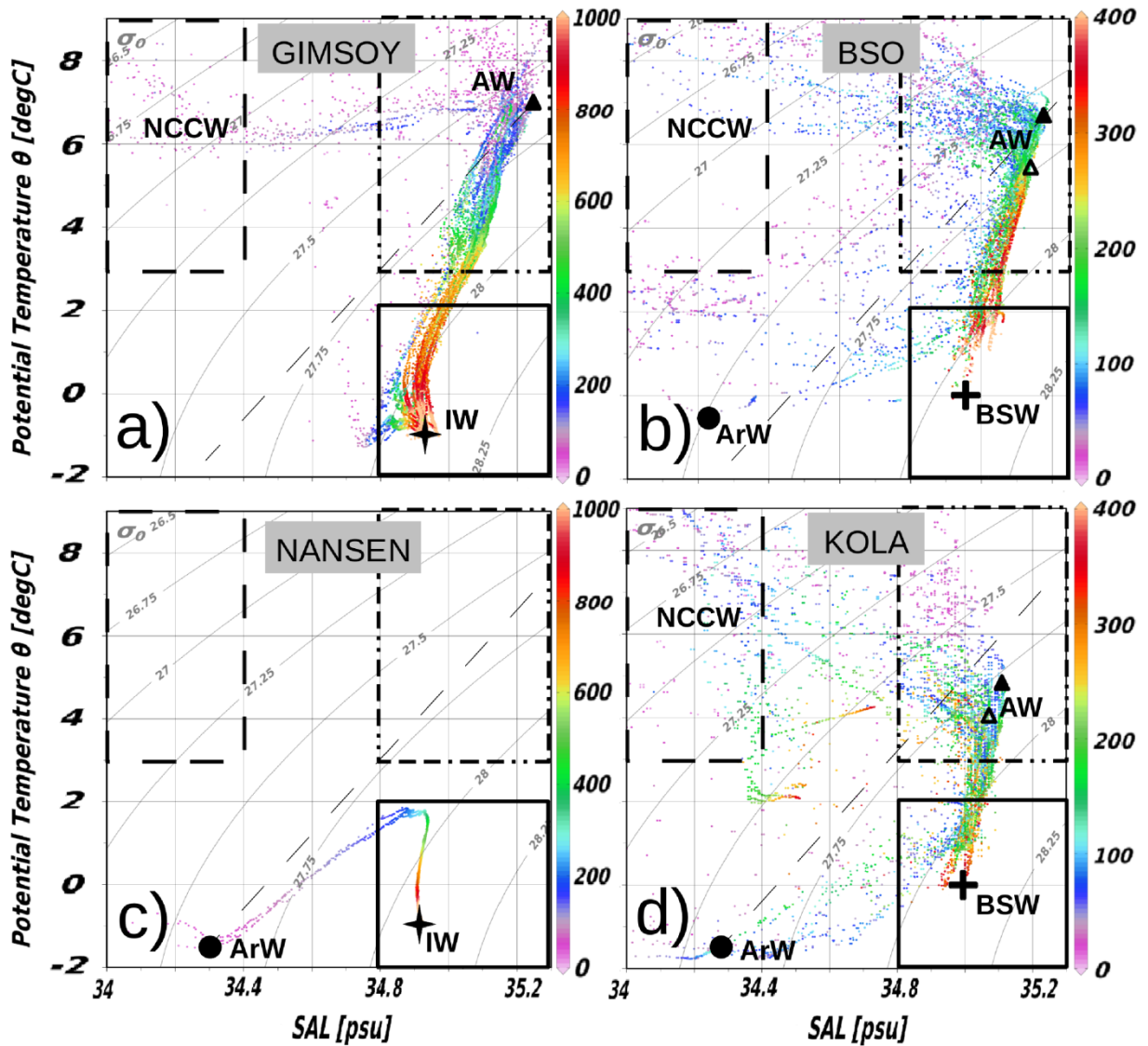


Figure 2: Potential temperature - Salinity Diagrams during summer the 1980-1985 period for: (a) Gimsoy section (b) BSO section (c) Nansen Bassin (d) KOLA setion. Filled triangles for summer Atlantic Waters (AW) and empty triangle for winter AW, star for Intermediate Waters (IW), cross for Barents Sea Waters (BSW) and circle for Arctic Waters (ArW). Dashed lines are mixing between ArW and AW.

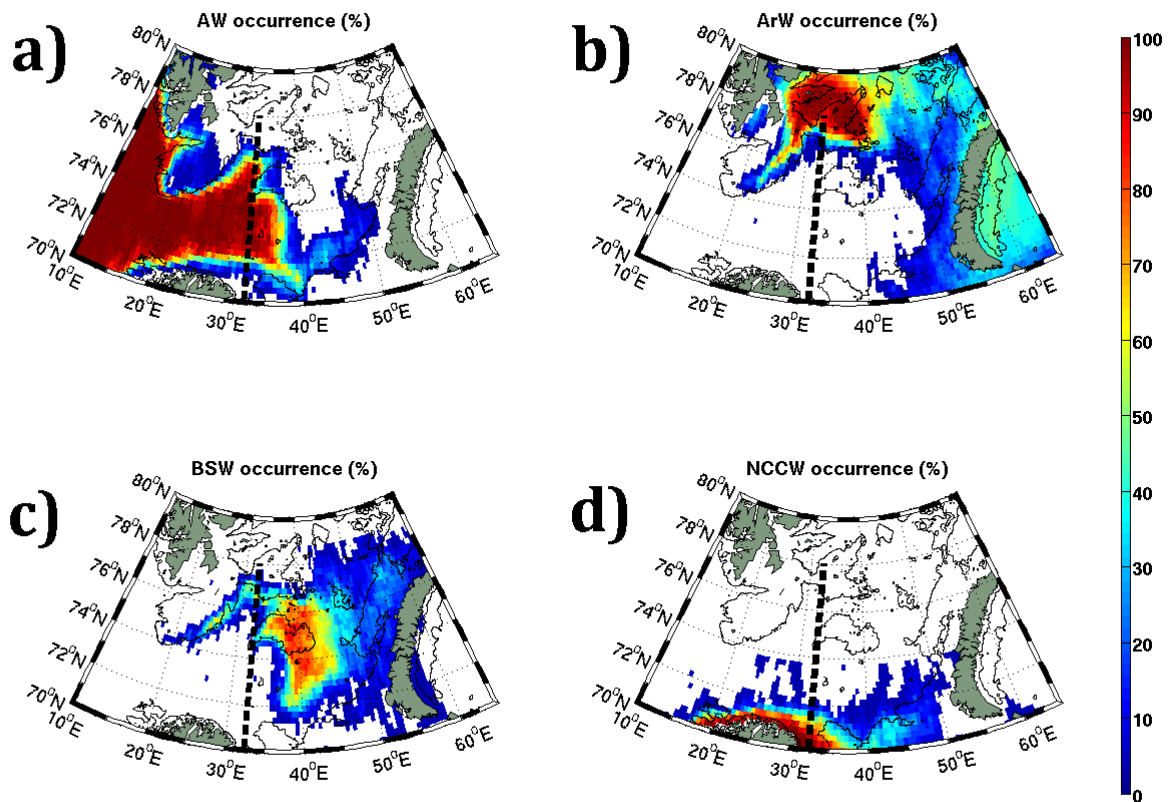


Figure 3 : Water Mass Occurrences over the 1980-2011 period (%) from the 50-100m layer during summer (august – september) for Atlantic Water (AW) (a), Arctic Water (ArW) (b), Barents Sea Water (BSW) (c), Coastal Water (CW) (d). KOLA Section in black dashed line. 200m isobaths is in black contours.

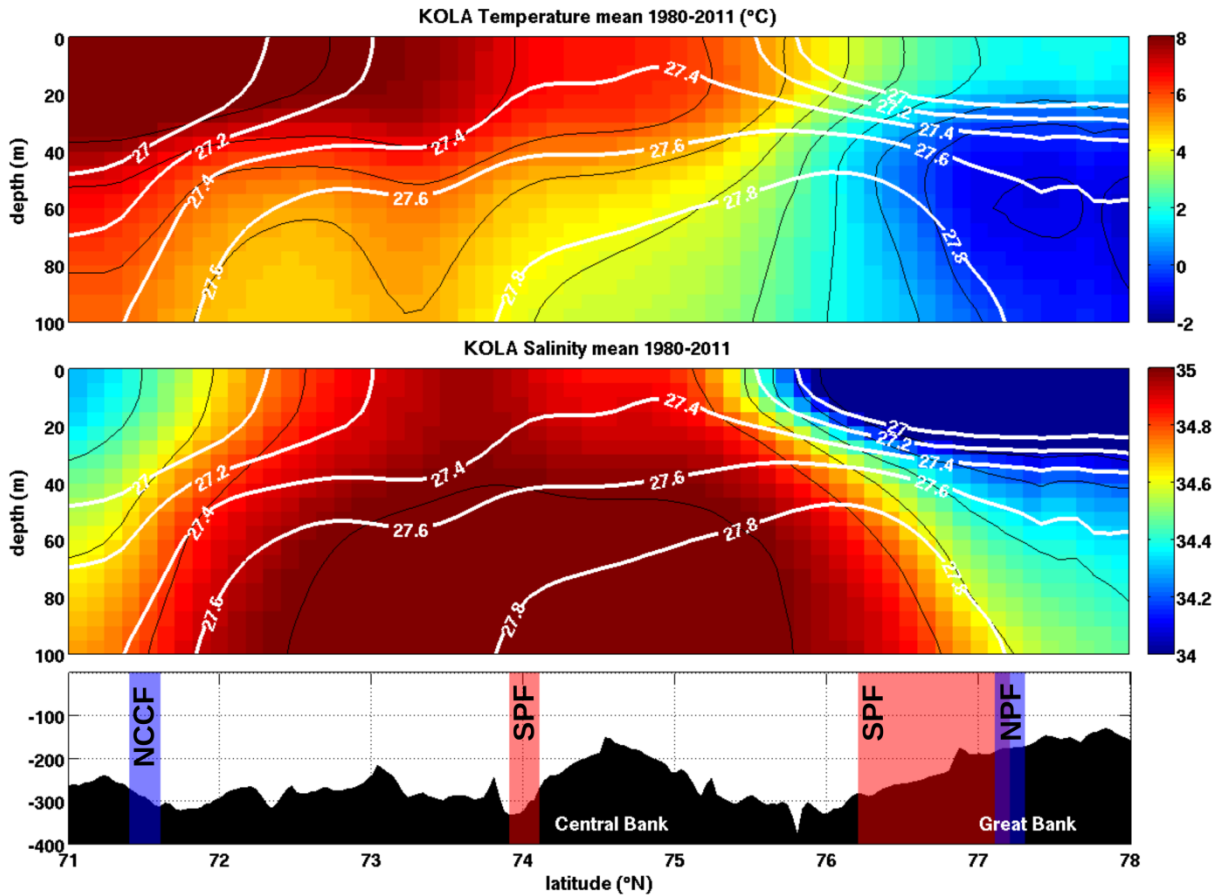


Figure 4 : Climatological summer (september) temperature (°C) (a), salinity (psu) (b) over the 1980-2011 from gridded in-situ data and bathymetry (c) at KOLA section. Isopycnals with equidistance of 0,1 kg/m³ are in white contours. Isotherms (top) and isohalines (bottom) with equidistances of 1°C and 0.1 psu respectively are marked in black. Maximum horizontal temperature and salinity gradients are in red and blue vertical lines respectively with corresponding fronts : Norwegian Coastal Current Front (NCCF), South Polar Front (SPF), North Polar Front (NPF).

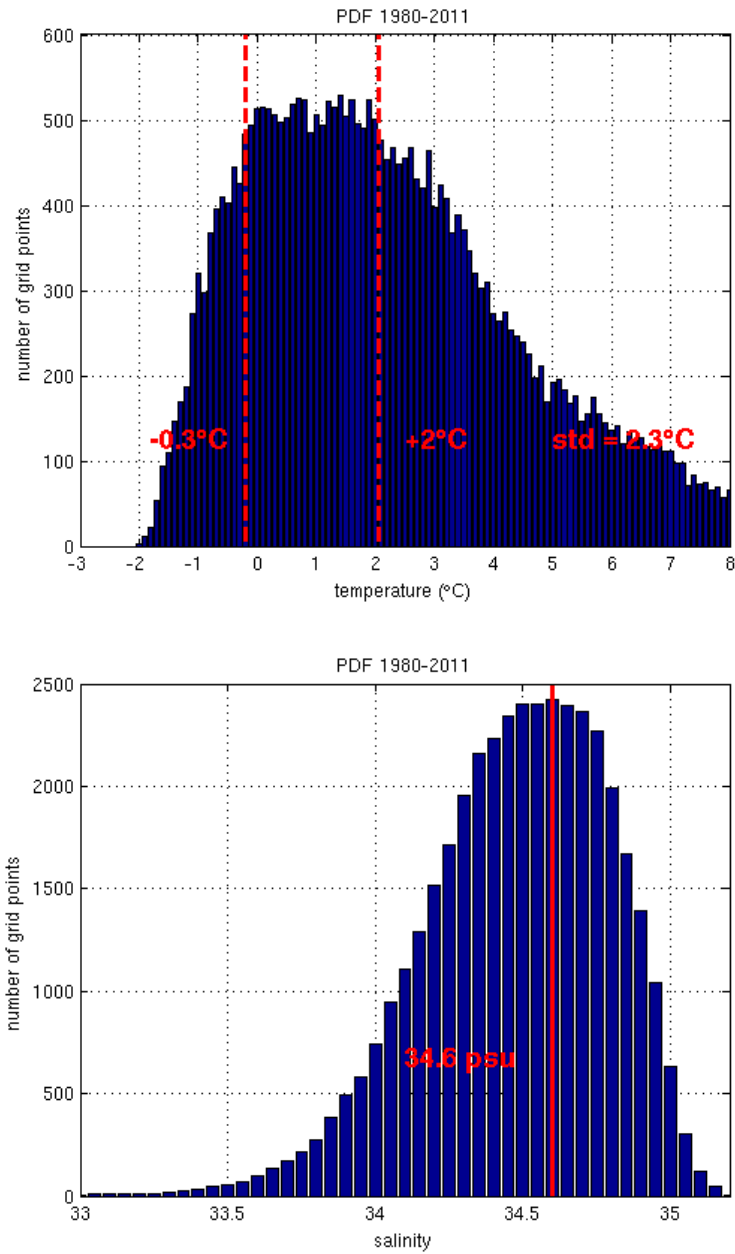


Figure 5 : Probability Density functions (PDF) of the temperature (a) and salinity (b) horizontal fields corresponding to large gradients averaged over the 1980-2011 summer periods. The Y-axis correspond to an area represented by number of grid point.

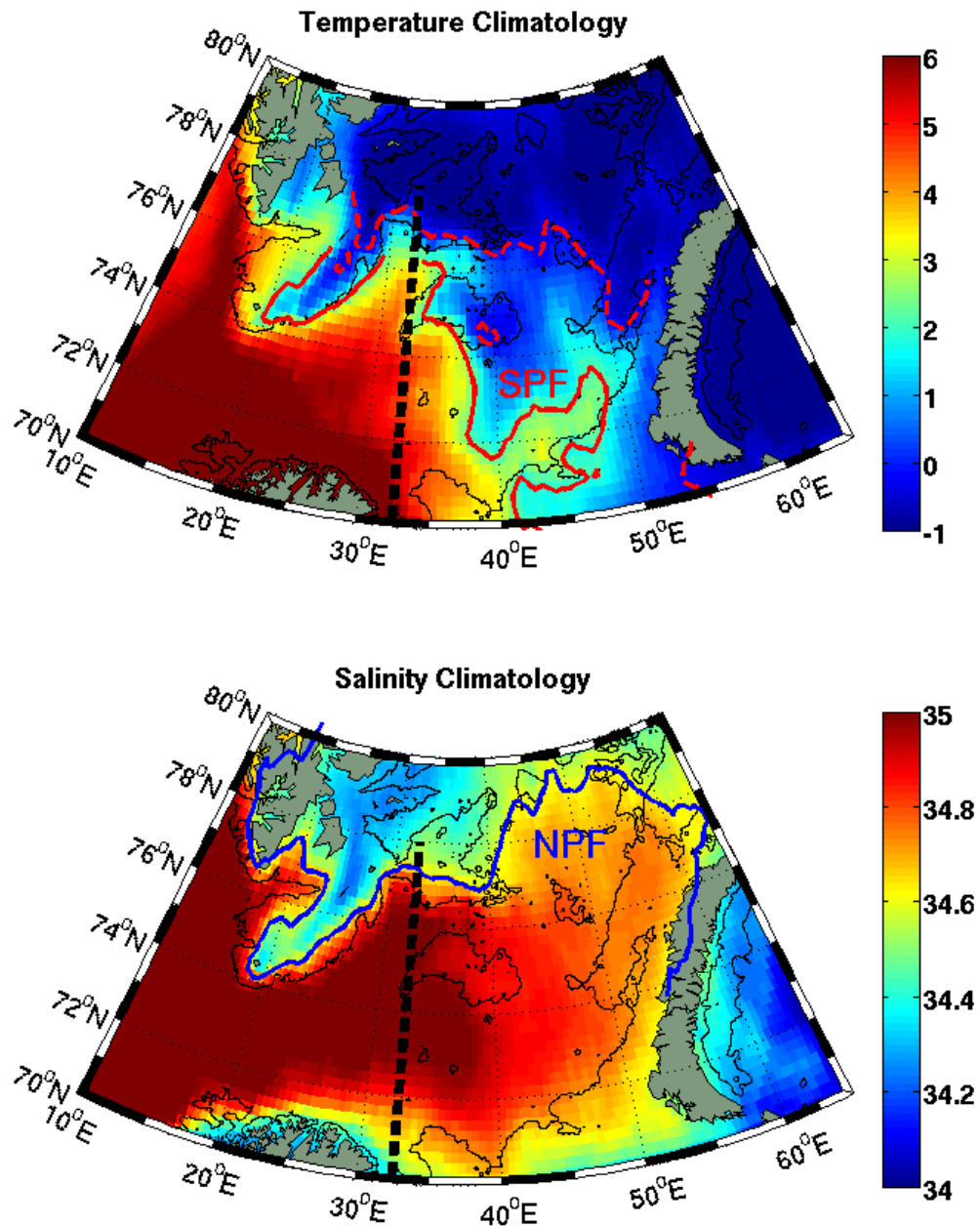


Figure 6 : Temperature (°C) (a) and Salinity (b) summer (august-september) climatology averaged over the 1980-2010 period for the 50-100m layer from in-situ gridded data. Temperature frontal zone in between solid thick red lines (SPF, +2°C isotherm) and dashed red line (-0,3°C isotherm). Salinity front in solid thick blue line (34,6 isohaline). KOLA Section in black dashed line. 200m isobath in black contours.

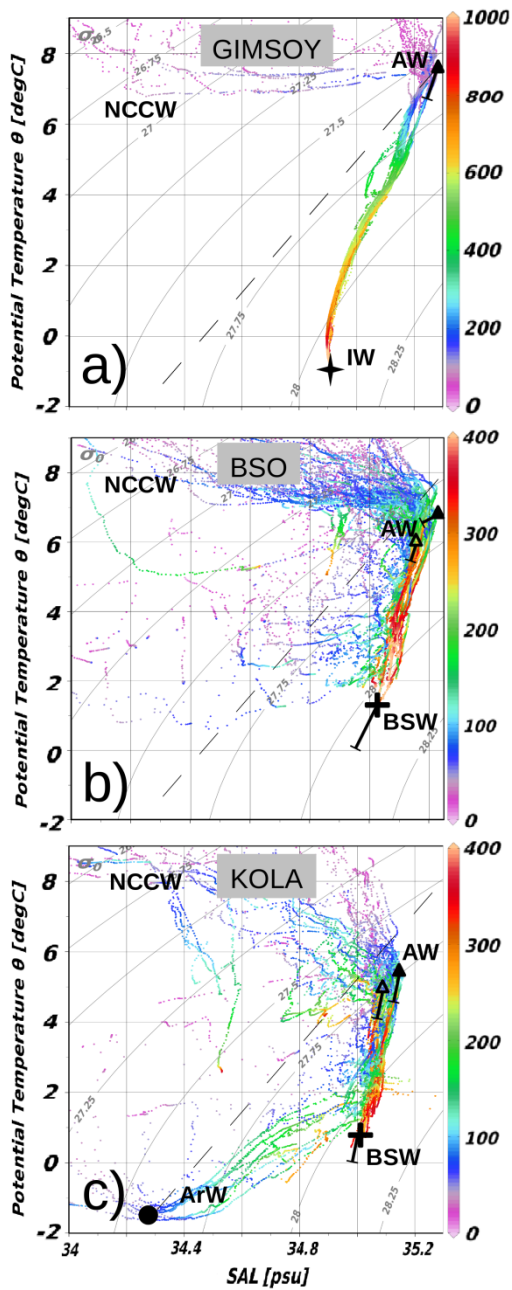


Figure 7 : Potential temperature - Salinity Diagrams during the summer 2005-2010 period and shifts in water mass characteristics from the summer 1980-1985 period for : (a) Gimsoy section (b) BSO section and (c) KOLA section. Triangles for Atlantic Waters upper (AW), star for Intermediate Waters (IW), cross for Barents Sea Waters (BSW) and circle for Arctic Waters (ArW). Dashed lines are mixing between ArW and AW.

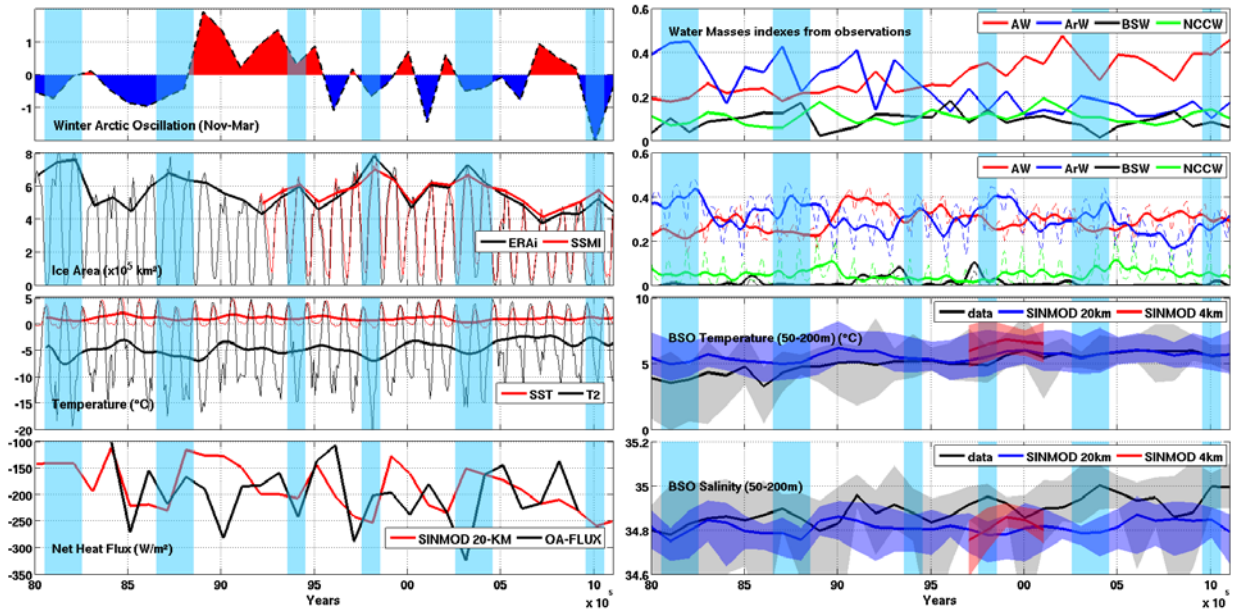


Figure8 : Inter-annual variations from 1980 to 2011 of :

(a) Winter Arctic Oscillation (November-March) from NOAA.

(b) BS Ice Area. From ERAi Re-analysis in black, from SSMI in red.

Thick lines are variations of the maximum sea Ice extent (March).

(c) BS air temperature at 2m & SST from ERAi Re-analysis.

Thick lines are low-passed signals (12 months).

(d) Heat Fluxes in the East Barents Sea from SINMOD 20km in red and OAFLUX in black.

(e) Water Masses index from In-situ observations and (f) from SINMOD 20km Outputs.

(g) BSO section temperature and (h) salinity (50-200m) from in-situ (black), SINMOD 20KM (blue) & SINMOD 4KM (red) data. Shady envelopes represent the seasonal variability of the time series.

Vertical bright blue lines are cold events.

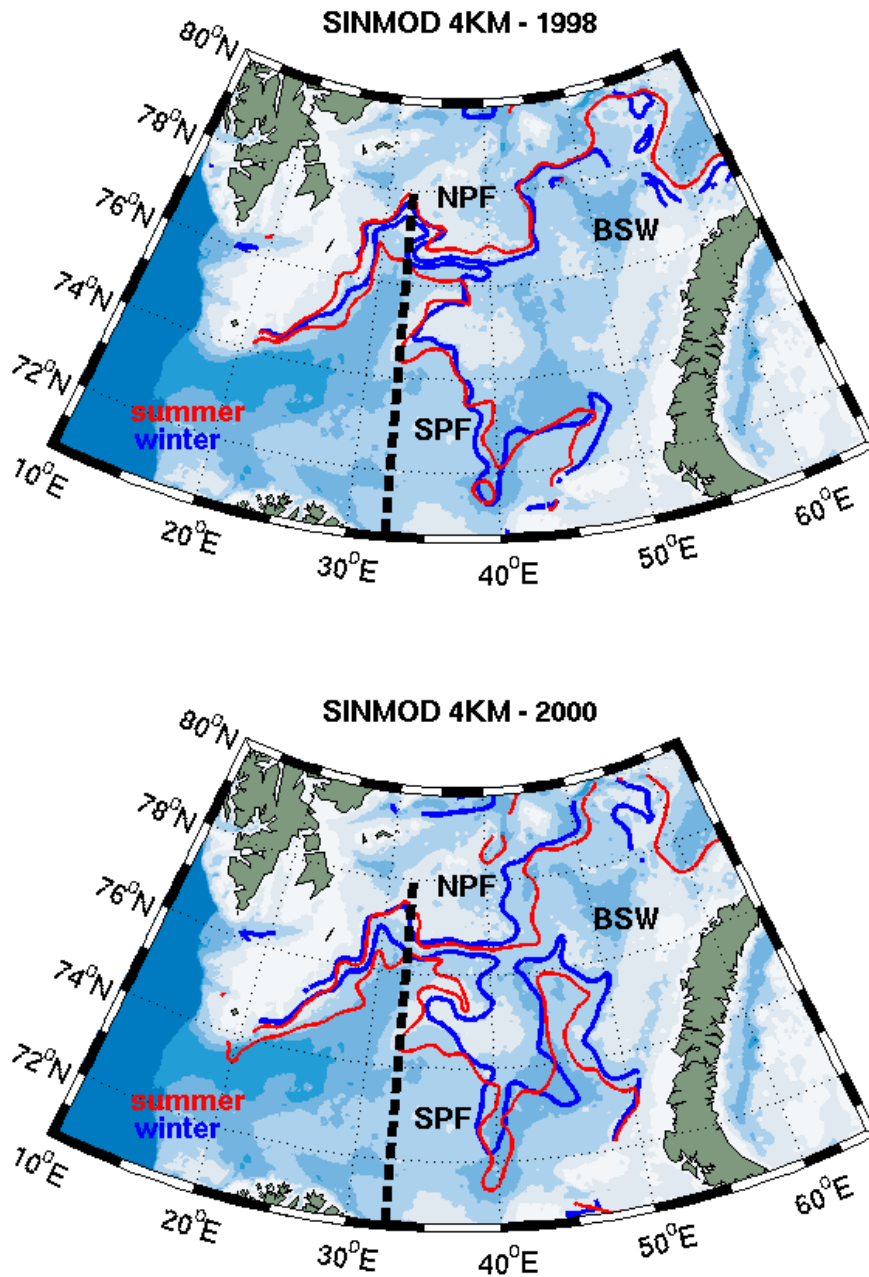


Figure 9 : Interannual and seasonal variability of SPF & NPF represented for summer (red) and winter (blue) between the cold 1998 (top) and the warm « Atlantified » 2000 (bottom). Bathymetry in the background. Barents Sea Waters (BSW) area in between the two fronts. KOLA Section in black dashed line.